



# Asian Journal of Scientific Research

ISSN 1992-1454

**science**  
alert  
<http://www.scialert.net>

**ANSI***net*  
an open access publisher  
<http://ansinet.com>

## A Numerical Study Laminar Forced Convection of Air for In-line Bundle of Cylinders Crossflow

<sup>1</sup>Tahseen A. Tahseen, <sup>1,2</sup>M. Ishak and <sup>1,2</sup>M.M. Rahman

<sup>1</sup>Faculty of Mechanical Engineering, University Malaysia Pahang, 26600 Pekan, Pahang, Malaysia

<sup>2</sup>Automotive Engineering Centre, Universiti Malaysia Pahang, 26600 Pekan, Pahang, Malaysia

*Corresponding Author: Tahseen A. Tahseen, Faculty of Mechanical Engineering, University Malaysia Pahang, 26600 Pekan, Pahang, Malaysia Tel: +609-424-2246*

### ABSTRACT

In the present study, the numerical analysis is two-dimensional steady state Navier-stokes equations and the energy equation governing laminar incompressible flow are solved using the Finite Difference Method (FDM) and the technique Body Fitted Coordinates (BFC). The constant heat flux is imposed on the surface of the tubes as the thermal boundary condition. The arrangement is considered in-line tube-banks the transverse ratio  $S_T/D$  and longitudinal pitch-to-diameter ratio  $S_L/D$  of 1.25, 1.75 and 2.25, respectively are also considered. Reynolds numbers of 30, 125 and 200 and Prandtl number is taken as 0.71. The temperature contours, local Nusselt number distributions at the tube surface and mean Nusselt number were analyzed in this study. It was found of that the strength of the heat transfer between the surface of tubes and the air flow increases with increasing Reynolds number and increasing pitch-to-diameter the ratio.

**Key words:** Cross-flow, finite difference, forced convection, circular in-line tube, body fitted coordinates

### INTRODUCTION

Heat transfer in flow across a bank of tubes is of importance in the design of many heat exchangers. Heat exchangers are found in numerous industrial applications, such as the condensers and evaporators of power plants, steam generation in a boiler, refrigerators or air cooling in the coil of an air conditioner and car radiators in which being compact, etc. Tube banks are usually arranged in an in-line or staggered manner and are characterized by the dimensionless transverse, longitudinal and diagonal pitches. Typically, one fluid moves over the tubes, while the other fluid, at a different temperature, passes through the tubes (Incropera *et al.*, 2007; Wang *et al.*, 2000; Zukauskas, 1972). The steady-state laminar incompressible flow across a tube bundle used a finite element method, has been introduced and applied to solve the two and three-dimensional energy equation and Navier-stokes equations by Arefmanesh and Alavi (2008), Dhaubhadel *et al.* (1986) and Fu and Tong (2002). Other researchers (Buyruk *et al.*, 1998; Fowler and Bejan, 2004) studied of the laminar heat transfer and fluid flow and pressure drop numerically and experimentally over a single tube and bundle of the parallel cylinder for low Reynolds number. The study optimization of a heat sink composed of parallel tubes in a solid matrix of fixed dimensions. The result validated, and complete numerical simulation was in the case stated by Canhoto and Reis (2011). The convective heat transfer and pressure drop in flow past two types

of the tube array is solved numerically by the finite analytic method. The tube arrays considered are in-line tube array and a staggered tube array with longitudinal and transverse pitch of two (Chen and Wung, 1989). Studied the effect of Reynolds number on flow and conjugate heat transfer in a high-performance inline and staggered arrangement of circular tubes bundle for a thermally and developing three-dimensional laminar flow, the range of Reynolds numbers  $300 = Re = 800$  (Jayavel and Tiwari, 2009). The investigate heat transfer from tube banks in cross-flow under an isothermal boundary condition. The control volume was selected from the fourth row of a tube as a typical cell to study the heat transfer from an in-line or staggered arrangement so, an analytical studies (Khan *et al.*, 2006). Studied the forced convection heat transfer for an incompressible, steady and Newtonian fluid flow over a bundle of circular cylinders has been investigated numerically. The momentum and energy equations have been solved by using a finite difference method (Juncu, 2007; Mandhani *et al.*, 2002). The two-dimensional numerical steady a cross flow over tube banks for the low Reynolds number study by Odabae and Hooman (2012), Wang *et al.* (2000) and Li *et al.* (2003). The effect along the splitter plate on the flow and heat transfer over a circular cylinder at low Reynolds numbers  $20 = Re = 1000$ . The result shows that the reduction in the drag coefficient as well as the observed average Nusselt number in the presence of the stability of the partition panel means of the area after accordingly and the reduction of vortex shedding. Also, heat transfer was increased conductor (Razavi *et al.*, 2008).

The numerical 2-D forced convection heat transfer for staggered tube banks in a cross flow was solved on the body fitted coordinates using the finite difference method for the flow over a bundle of circular tubes. The ratio  $S_T/D$  of 1.25, 1.5 and 2.0 is also considered. Reynolds numbers are varied between 25-250 and Prandtl number is taken as 0.71 (Tahseen *et al.*, 2011). A two dimensional laminar flow past a square cylinder and row of cylinders by using the Lattice Boltzmann Method (LBM) proposed by Islam and Zhou (2009) and Ul-Islam and Zhou (2009). The first research the different Reynolds numbers with the different distance between the cylinders and second keep the Reynolds number 100 for all study. A naphthalene sublimation technique was employed to obtain the local heat transfer coefficients, and the experiment was performed for various tube spacing, tube locations and Reynolds numbers. The average Nusselt number increases more than 30% and 65% on the second and third tubes, respectively, in comparison with that of the first tube. Also the empirical correlations for average heat transfer coefficients are compared with the conventional heat transfer correlations (Yoo *et al.*, 2007). A tube banks has been studied for fluid flow and heat transfer by many researchers in the past.

This study is heat transfer over circular in-line tube for the three Reynolds number with the change of transverse and longitudinal pitch to tube diameter ratios and heat fluxes in tube surface. Consideration is given to the two-dimension steady laminar incompressible flow.

## **MATERIALS AND METHODS**

The treated problem is a two-dimensional of an in-line tube bank with the diameter of tube 10 mm. The equations governing the conservation of continuity, momentum and energy equation. The basic flow configuration with two-dimensional, laminar, steady, constant fluid properties and incompressible. The physical system considered in the present study is displayed in Fig. 1. The governing equations were transformed into dimensionless forms upon incorporating the following non-dimensional variables:

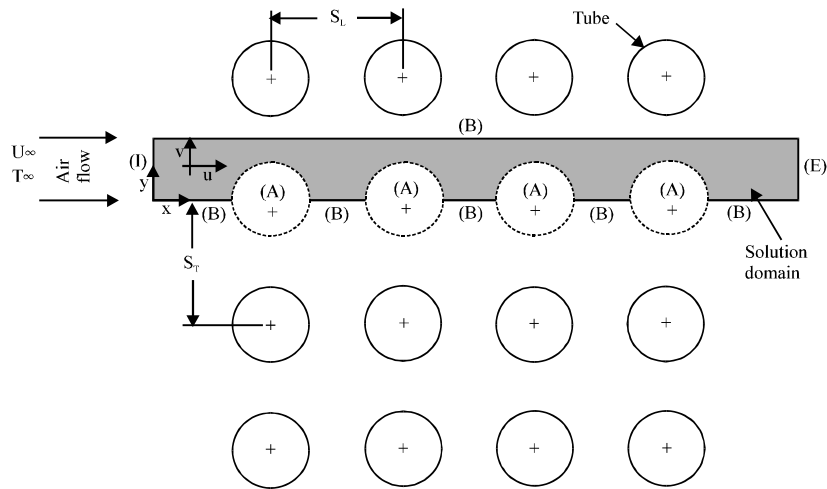


Fig. 1: In-line tube bank nomenclature: (a) Tube arrangements, (b) Solution domain

$$(X, Y) = \frac{(x, y)}{D}, P = \frac{p}{\rho U_\infty^2}, (U, V) = \frac{(u, v)}{U_\infty}, \theta = \frac{T - T_\infty}{T_w - T_\infty}, Re_D = \frac{U_\infty D}{\nu}, Pr = \frac{\mu C_p}{k} \quad (1)$$

where, X and Y are the dimensionless coordinates measured along the horizontal and vertical axes, respectively. The u and v being the dimensional velocity components along x- and y-axes, and  $\theta$  is the dimensionless temperature. The dimensionless forms of the governing equations under steady state condition are expressed in the following forms (Bejan, 2004):

- Continuity:

$$\frac{\partial U}{\partial X} + \frac{\partial V}{\partial Y} = 0 \quad (2)$$

- Momentum (Navier-stokes):

$$\left. \begin{aligned} U \frac{\partial V}{\partial X} + V \frac{\partial V}{\partial Y} &= -\frac{\partial P}{\partial X} + \frac{1}{Re_D} \left[ \frac{\partial^2 U}{\partial X^2} + \frac{\partial^2 U}{\partial Y^2} \right] \\ U \frac{\partial V}{\partial X} + V \frac{\partial V}{\partial Y} &= -\frac{\partial P}{\partial X} + \frac{1}{Re_D} \left[ \frac{\partial^2 V}{\partial X^2} + \frac{\partial^2 V}{\partial Y^2} \right] \end{aligned} \right\} \quad (3)$$

- Energy:

$$U \frac{\partial \theta}{\partial X} + V \frac{\partial \theta}{\partial Y} = \frac{1}{Pr Re_D} \left[ \frac{\partial^2 \theta}{\partial X^2} + \frac{\partial^2 \theta}{\partial Y^2} \right] \quad (4)$$

The schematic of an in-line tube banks and computational domain is shown in Fig. 1. The boundary conditions used for the solution domain are uniform inlet velocity, fully developed out flow and a combination of symmetry and no-slip tube surfaces on the bottom and top boundaries. The boundary conditions prescribed for U, V and  $\theta$  are summarized in Table 1.

Table 1: The boundary conditions for U, V and  $\theta$

		U	V	$\theta$
A	Tube surface	0	0	1
B	Symmetry	$\partial U/\partial Y = 0$	0	$\partial \theta/\partial Y = 0$
I	Inlet ( $x = 0$ )	1	0	0
E	Exit	$\partial U/\partial X = 0$	0	0

The heat transfer coefficient  $h$ , can be expressed in the dimensionless form by the local and average Nusselt numbers  $Nu$  and  $\bar{Nu}$ , which is defined as Eq. 5 and 6, respectively (Chen and Wung, 1989):

$$Nu = \frac{hD}{k} = - \left. \frac{\partial \theta}{\partial n} \right|_{\phi} \quad (5)$$

$$\bar{Nu} = \frac{\bar{h}D}{k} = \left( \int_{\phi} Nu \, ds \right) / \left( \int_{\phi} ds \right) \quad (6)$$

where,  $h$  and  $\bar{h}$  are the local and mean heat transfer coefficients,  $ds$  are the infinitesimal distance on the contour and  $\phi$  of the tube wall.

The set of conservation (Eq. 3 and 4) can be written in general form in Cartesian coordinates as Eq. 7:

$$\frac{\partial(U\phi)}{\partial X} + \frac{\partial(V\phi)}{\partial Y} = \frac{\partial}{\partial X} \left( \Gamma \frac{\partial \phi}{\partial X} \right) + \frac{\partial}{\partial Y} \left( \Gamma \frac{\partial \phi}{\partial Y} \right) + S_{\phi} \quad (7)$$

where, the effective diffusion coefficient  $\Gamma$ , the general dependent variable  $\phi$  and the source term  $S_{\phi}$ . The continuity equation, Equation 2 has no diffusion and source terms. It will be used to derive an equation for the pressure correction. The grid generation scheme based on elliptic partial differential equations is used in the present study to generate the curvilinear coordinates. Equation 7 can be transformed from the physical domain to the computational domain according to the following transformation  $\zeta = \zeta(x,y)$ ,  $\eta = \eta(x,y)$  (Thompson *et al.*, 1997). The final form of the transformed equation can be written as Eq. 8:

$$\frac{\partial}{\partial \zeta} (\phi G_1) + \frac{\partial}{\partial \eta} (\phi G_2) = \frac{\partial}{\partial \zeta} \left( \frac{\Gamma}{J} \left( \alpha \frac{\partial \phi}{\partial \zeta} - \gamma \frac{\partial \phi}{\partial \eta} \right) \right) + \frac{\partial}{\partial \eta} \left( \frac{\Gamma}{J} \left( \beta \frac{\partial \phi}{\partial \eta} - \gamma \frac{\partial \phi}{\partial \zeta} \right) \right) + JS_{\phi} \quad (8)$$

where,  $G_1$  and  $G_2$  are the contravariant velocity components,  $J$  is the Jacobian of the transformation on the computational plane and  $\alpha$ ,  $\beta$ ,  $\gamma$  are the coefficients of transformation. They are expressed as:

$$\left. \begin{aligned} G_1 &= U \frac{\partial Y}{\partial \eta} - V \frac{\partial X}{\partial \eta}, \quad G_2 = V \frac{\partial X}{\partial \zeta} - U \frac{\partial Y}{\partial \zeta}, \quad J = \left( \frac{\partial X}{\partial \zeta} \frac{\partial Y}{\partial \eta} - \frac{\partial Y}{\partial \zeta} \frac{\partial X}{\partial \eta} \right) \\ \alpha &= \left( \frac{\partial x}{\partial \eta} \right)^2 + \left( \frac{\partial y}{\partial \eta} \right)^2, \quad \gamma = \left( \frac{\partial x}{\partial \zeta} \frac{\partial x}{\partial \eta} \right) + \left( \frac{\partial y}{\partial \zeta} \frac{\partial y}{\partial \eta} \right), \quad \beta = \left( \frac{\partial x}{\partial \zeta} \right)^2 + \left( \frac{\partial y}{\partial \zeta} \right)^2 \end{aligned} \right\} \quad (9)$$

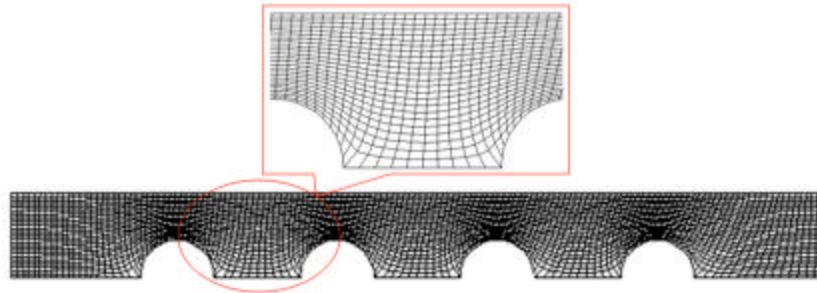


Fig. 2: Schematic of grid systems generated by Body-Fitted Coordinates (BFC)

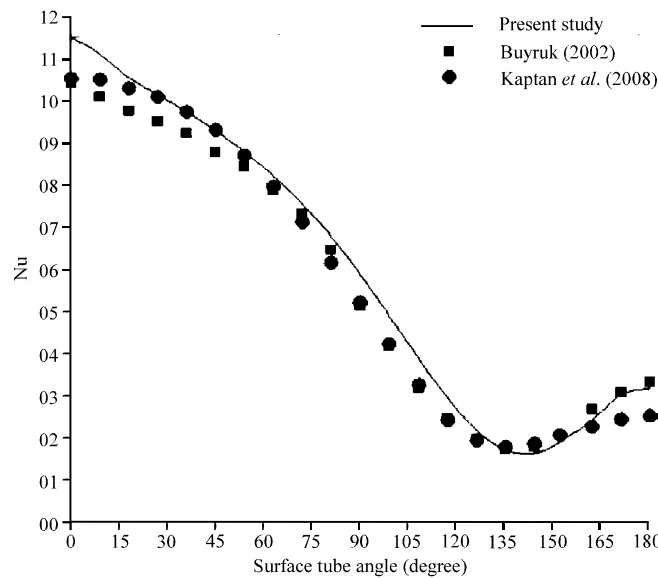


Fig. 3: Comparison between the present study with previous literatures (Buyruk, 2002; Kaptan *et al.*, 2008) for local Nusselt number with  $Re = 120$ ,  $Pr = 0.71$  and  $S_T/D = 2.0$

Equation 8 was solved numerically using a control volume-based finite volume method. The solved by the marching type procedure involving a series of the two-dimensional elliptic problem in the cross-stream plane. The marching step size is  $1 \times 10^{-4}$  along the axial distance. At each marching step, the strong coupling of pressure and velocity in the cross section was calculated by the Simple-algorithm on a collocated non-orthogonal grid. It is used to adjust the velocity field to satisfy the conservation of mass (Patankar, 1980). For the computational calculations, a computer code was prepared in FORTRAN-90. In the numerical calculation, the  $146 \times 25$  grid arrangements are found to be sufficient for grid independent solution and then the 2D-algebraic, Fig. 2 show the grid generation used the body fitted coordinate.

**Validation:** The numerical model was validated with some of the previous published benchmark problems. The air flow and heat transfer over in-line circular tube subjected to constant heat flux were predicted. The Nusselt number for the fully developed region between two tubes subjected to constant wall temperature. Figure 3 shows the comparison between the present study with previous

literatures (Buyruk, 2002; Kaptan *et al.*, 2008) for local Nusselt number with  $Re = 120$ ,  $Pr = 0.71$  and  $S_T/D = 2.0$ . It can be seen that an excellent agreement is achieved between the present results and the numerical results of Buyruk (2002) and Kaptan *et al.* (2008) and for the local Nusselt number distribution circumference of the first tube.

## RESULTS AND DISCUSSION

Here, the numerical solutions of laminar forced convection heat transfer across tube bundles with in-line arrays is presented. The transverse pitch to tube diameter ratios ( $S_T/D$ ), of 1.25, 1.75 and 2.25 and the longitudinal  $S_T/D = S_L/D$ . They are considered in the flow fields of  $Re = 30$ , 125 and 200. A heat flux in the surface tubes also varies of 50, 100 and  $190 \text{ W m}^{-2}$ . The normalized temperature (isotherms), all isotherms are ranging from 0 to 1 that represents a low air temperature at the inlet to higher air temperature as it reaches the hot tube surface.

Figure 4 shows the effect of heat flux on isotherms for the three modules for  $Re = 125$  and  $S_T/D = 1.75$ . A general view of the floods, also increases the value of the  $Re$  number of lower value isotherms penetrate deeper, which means that the cold air near the hot surface. It is clear, that the hot layer thickness increases with increases heat flux. Also, Fig. 5 show the effect of the transverse  $S_T/D$  on isotherms for the three modules 1.25, 1.75 and 2.25 at  $Re = 200$  and heat flux =  $190 \text{ W m}^{-2}$ .

Figure 6 presents the relationship between the local Nusselt number and the surface tube angle for various Reynolds numbers at all half location of the tube. A laminar boundary layer develops from the front stagnation point for a cylinder in cross-flow and grows in thickness around the circular tube. The maximum heat transfer rate is located close to the front stagnation point and the local Nusselt number decreases with the angle. The position of the minimum local Nusselt number is not fixed around 162 deg. at  $Re = 30$ , 153 deg. at  $Re = 125$  and 145 deg. at  $Re = 200$ . It is noted that the maximum values in the first tube and drop to minimum values of local Nusselt number a rein the fourth tube. This is due to the cold air when to stick to the first tube hot. Thus, the difference in temperature a large and thus the heat transfer coefficient is the maximum value, because it depends on the difference in temperature between the tube surface and the air flow. The air flow when it passes over the first tube it is gaining heat. Thus, the temperature difference between the second tube and the air flow will be less. Thus, the heat transfer coefficient will be less and so also for the third and fourth tube. As for why the heat transfer coefficient of the surfaces at the beginning of small and then begins to increase, this is due to the hot layer may be

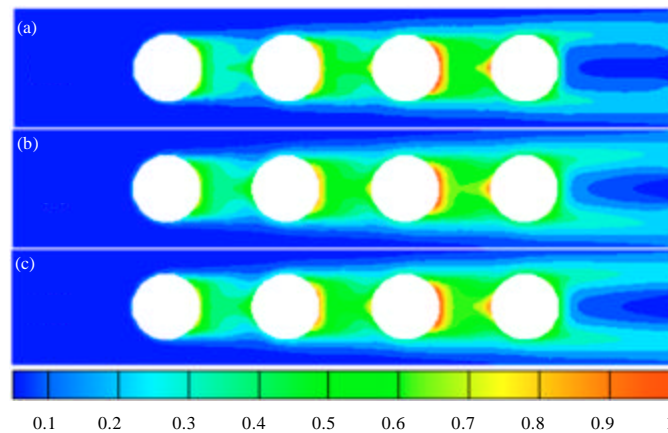


Fig. 4(a-c): Effect of heat flux on isotherms for the three modules, Reynolds number = 125 and  $S_T/D = 1.75$ : (a) 50, (b) 100 and (c)  $190 \text{ W m}^{-2}$

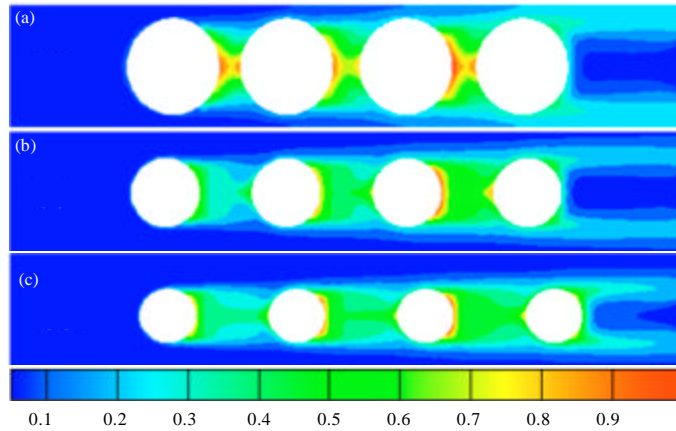


Fig. 5(a-c): Effect of the transverse  $S_T/D$  on isotherms for the three modules, Reynolds number = 200 and heat flux =  $190 \text{ W m}^{-2}$ : (a) 1.25, (b) 1.75 and (c) 2.25

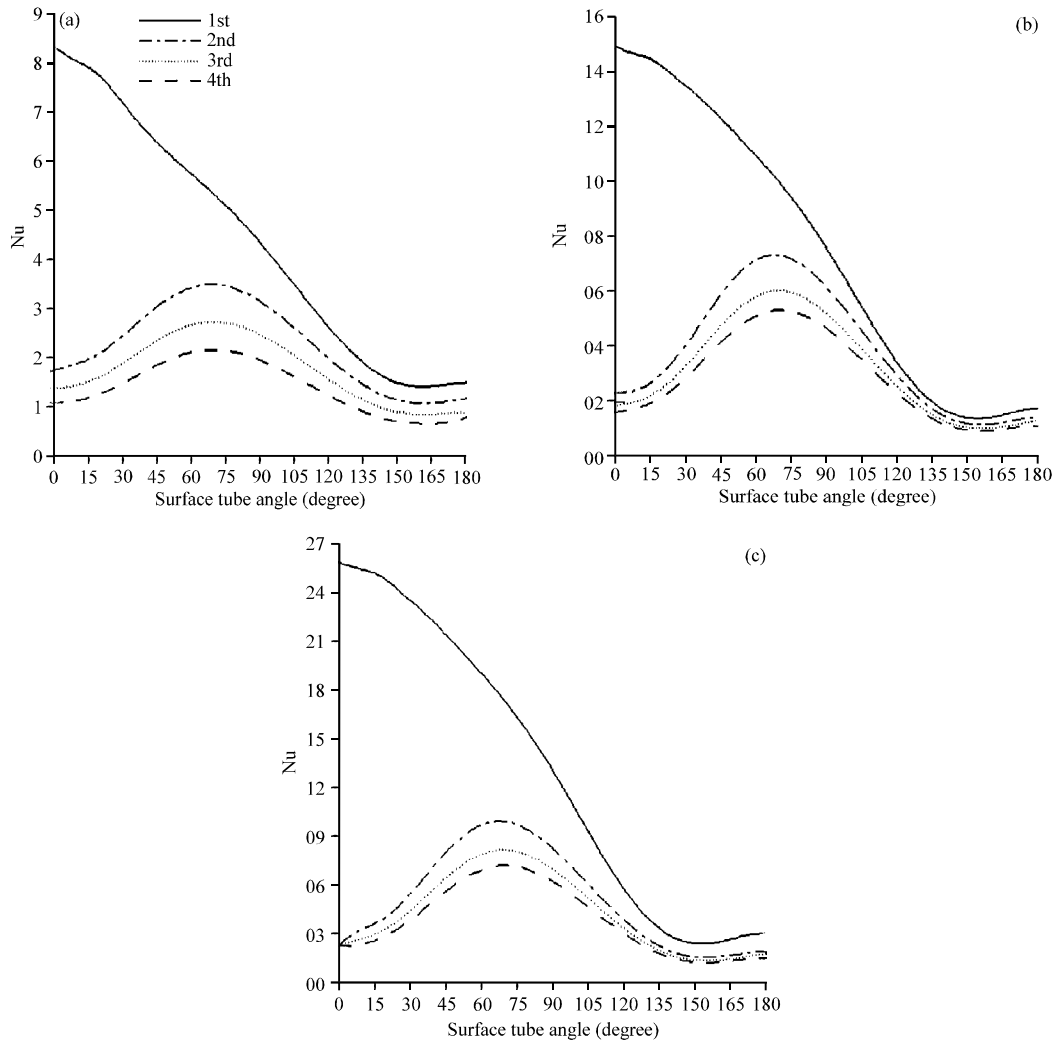


Fig. 6(a-c): Surface local Nusselt number distribution with  $S_T/D = 1.75$  for Reynolds number of (a) 30, (b) 125 and (c) 200



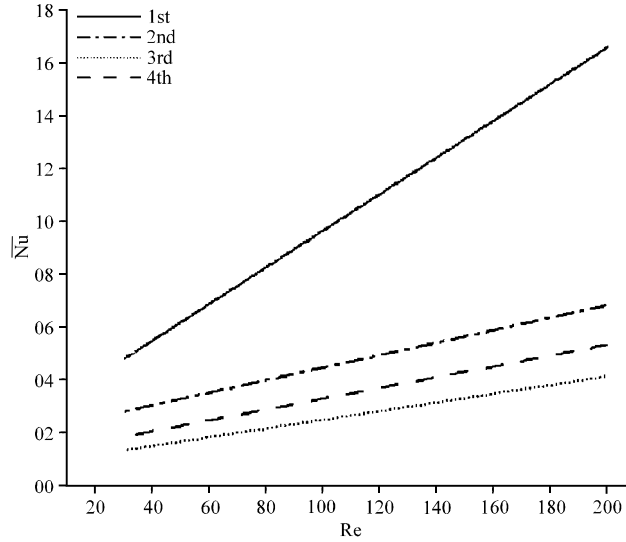


Fig. 7: Effect of Reynolds number on average Nusselt number for  $S_T/D = 2.25$  at  $Pr = 0.71$

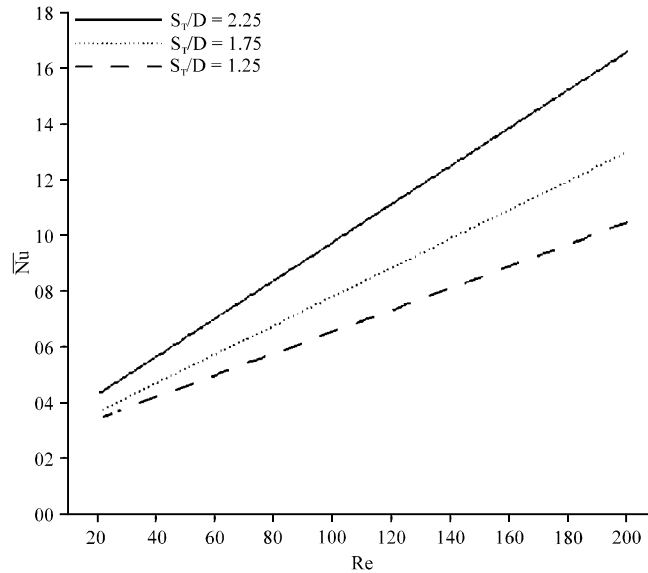


Fig. 8: Effect of Reynolds number on average Nusselt number with different  $S_T/D$  for the first tube at  $Pr = 0.71$

continuous between the tubes. The increase in the heat transfer coefficient between the angles 60 and 90 deg. because the temperature, of the air flow when the current is less than the area values to them.

Figure 7 shows typical examples of a variation of the mean Nusselt number ( $\overline{Nu}$ ) with the Reynolds number for  $Pr = 0.71$ . Represented in this figure are the result at  $S_T/D = 2.25$ . It is clear that  $\overline{Nu}$  number, increases almost linearly with Re number. In general, the maximum value of the  $\overline{Nu}$  is keep at the first tube. While the small values of mean Nusselt number be relatively for the other tubes also, converge values and take the same action-oriented.

Figure 8 shows the relation of  $\overline{Nu}$  number and Re number for the first tube at  $Pr = 0.71$ . It can be seen that the  $\overline{Nu}$  number increased with the increase of Re number as well as the pitch-to

diameter ratio  $S_p/D$ . However, further increase of the pitch-to diameter ratio will to additional improvement in heat transfer.

## CONCLUSION

In this study, the BFC method was adopted to generate 2-D computational grids, then the tube surface from side heat transfer air flow. The numerical results of local Nusselt number and temperature distributions on air flow and the average Nusselt number were studied. The study results can be summarized as:

- As the local Nusselt number decreases rapidly along the flow direction, at the outlet region. It is much smaller compared with the values of the entrance region to the back of the tube
- The maximum value of local Nusselt numbers in first tube at the all transverse pitch
- As the average Nusselt number of air flow increases with the increase of Reynolds number
- Finally, transverse and longitudinal pitch is increased, the average Nusselt number increase

## ACKNOWLEDGMENTS

This research under study of the Ph.D. in Mechanical Engineering. The authors would like to thank the Faculty of Mechanical Engineering in Universiti Malaysia Pahang (UMP) and Universiti Malaysia Pahang for financial support under RDU110332. The first author is grateful to the assistance of Dr. Ahmed W. Mustafa (Tikrit University-Iraq).

## REFERENCES

- Arefmanesh, A. and M.A. Alavi, 2008. A hybrid finite difference-finite element method for solving the 3D energy equation in non-isothermal flow past over a tube. *Int. J. Numerical Methods Heat Fluid Flow*, 18: 50-66.
- Bejan, A., 2004. *Convection Heat Transfer*. 3rd Edn., John Wiley and Sons Inc., Hoboken, New Jersey.
- Buyruk, E., 2002. Numerical study of heat transfer characteristics on tandem cylinders, inline and a staggered tube banks in cross-flow of air. *Int. Comm. Heat Mass Transfer*, 29: 355-366.
- Buyruk, E., M.W. Johnson and I. Owen, 1998. Numerical and experimental study of flow and heat transfer around a tube in cross-flow at low Reynolds number. *Int. J. Heat Fluid Flow*, 19: 223-232.
- Canhoto, P. and A.H. Reis, 2011. Optimization of fluid flow and internal geometric structure of volumes cooled by forced convection in an array of parallel tubes. *Int. J. Heat Mass Trans.*, 54: 4288-4299.
- Chen, C.J. and T.S. Wung, 1989. Finite analytic solution of convective heat transfer for tube arrays in crossflow: Part II-heat transfer analysis. *J. Heat Transfer*, 111: 641-648.
- Dhaubhadel, M.N., J.N. Reddy and D.P. Telionis, 1986. Penalty finite-element analysis of coupled fluid flow and heat transfer for in-line bundle of cylinders in cross flow. *Int. J. Non-Linear Mech.*, 21: 361-373.
- Fowler, A.J. and A. Bejan, 1994. Forced convection in banks of inclined cylinders at low Reynolds numbers. *Int. J. Heat Fluid Flow*, 15: 90-99.
- Fu, W.S. and B.H. Tong, 2002. Numerical investigation of heat transfer from a heated oscillating cylinder in a cross flow. *Int. J. Heat Mass Trans.*, 45: 3033-3043.
- Incropera, F.P., D.P. Dewitt, T.L. Bergman and A.S. Lavine, 2007. *Fundamentals of Heat and Mass Transfer*. 6th Edn., Wiley, New York, pp: 152-155.

- Islam, S.U. and C.Y. Zhou, 2009. Numerical simulation of flow around a row of circular cylinders using the lattice boltzmann method. *Inform. Technol. J.*, 8: 513-520.
- Jayavel, S. and S. Tiwari, 2009. Numerical study of heat transfer and pressure drop for flow past inline and staggered tube bundles. *Int. J. Numerical Methods Heat Fluid Flow*, 19: 931-949.
- Juncu, G., 2007. A numerical study of momentum and forced convection heat transfer around two tandem circular cylinders at low Reynolds numbers. Part I: momentum transfer. *Int. J. Heat Mass Trans.*, 50: 3799-3808.
- Kaptan, Y., E. Buyruk, and A. Ecdar, 2008. Numerical investigation of fouling on cross-flow heat exchanger tubes with conjugated heat transfer approach. *Int. Comm. Heat Mass Trans.*, 35: 1153-1158.
- Khan, W.A., J.R. Culham and M.M. Yovanovich, 2006. Convection heat transfer from tube banks in cross flow: Analytical approach. *Int. J. Heat Mass Trans.*, 49: 4831-4838.
- Li, T., N.G. Deen and J.A.M. Kuipers, 2003. Numerical study of hydrodynamics and mass transfer of in line fiber arrays in laminar cross-flow. *Proceedings of the 3rd International Conference on CFD in the Minerals and Process Industries CSIRO, December 10-12, 2003, Melbourne, Australia.*
- Mandhani, V.K., R.P. Chhabra and V. Eswaran, 2002. Forced convection heat transfer in tube banks in cross flow. *Chemical Eng. Sci.*, 57: 379-391.
- Odabae, M. and K. Hooman, 2012. Metal foam heat exchangers for heat transfer augmentation from a tube bank. *Applied Thermal Eng.*, 36: 456-463.
- Patankar, S.V., 1980. *Numerical Heat Transfer and Fluid Flow*. Hemisphere Publishing Corporation, New York.
- Razavi, S.E., F. Vahid and B. Farzad, 2008. Impact of a splitter plate on flow and heat transfer around circular cylinder at low Reynolds numbers. *J. Applied Sci.*, 8: 1286-1292.
- Tahseen, T.A., M. Ishak and M.M. Rahman, 2011. A numerical study of forced convection heat transfer for staggered tube banks in cross-flow. *Proceedings of the 1st International Conference of Mechanical Engineering Research, December 5-7, 2011, Pahang, Malaysia*, pp: 216-227.
- Thompson, J.F., Z.U.A. Warsi and C.W. Martin, 1997. *Numerical Grid Generation, Foundations and Applications*. North-Holland, New York.
- Ul-Islam, S., and C.Y. Zhou, 2009. Characteristics of flow past a square cylinder using the lattice boltzmann method. *Inform. Technol. J.*, 8: 1094-1114.
- Wang, Y.Q., L.A. Penner and S.J. Ormiston, 2000. Analysis of laminar forced convection of air for crossflow in banks of staggered tubes. *Numerical Heat Transfer, Part A*, 38: 819-845.
- Yoo, S.Y., H.K. Kwon and J.H. Kim, 2007. A study on heat transfer characteristics for staggered tube banks in cross-flow. *J. Mech. Sci. Technol.*, 21: 505-512.
- Zukauskas, A., 1972. Heat transfer from tubes in crossflow. *Adv. Heat Transfer*, 8: 93-158.